Springer

Journal of
Mechanical
Science and
Technology

Journal of Mechanical Science and Technology 22 (2008) 931~936

www.springerlink.com/content/1738-494x

Processing map for the hot working of Ti-8Ta-3Nb

Kyung Won Lee[1,*], Jae Sam Ban[2], Min Geun Lee[1], Gyu Ha Kim[3] and Kyu Zong Cho[4]

[1]*Department of Mechanical Engineering, Chonnam National University, Gwangju 500-757, Korea*
[2]*LED/LD Packaging Service Center, Gwangju 500-470, Korea*
[3]*Professor, Division of Automotive & Mechanical Engineering, Nambu University, Gwangju 506-824, Korea*
[4]*Professor, Department of Mechanical Engineering, Chonnam National University, Gwangju 500-757, Korea*

(Manuscript Received July 19, 2007; Revised January 7, 2008; Accepted January 9, 2008)

Abstract

This paper considers the deformation behavior during hot forging in as-cast and forged specimens of Ti-8Ta-3Nb. The experimental specimens are as-cast and forged specimens of Ti-8Ta-3Nb. The deformation behavior of Ti-8Ta-3Nb alloy has been characterized on the basis of its flow stress variation obtained by true strain rate compression testing in the temperature range 650-900℃ and strain rate range 0.001-10s^{-1}. The present study aims at assessing the hot workability of as-cast and forged Ti-8Ta-3Nb using the approach of processing maps and comparing specimens of Ti-8Ta-3Nb. The maps are an explicit representation of the various processes that occur in the different temperature and strain rate conditions. The construction of the maps is based on the experimentally determined changes of strain rate sensitivity coefficient. Processing maps were obtained at strains of 0.2, 0.3, 0.4 and 0.5 in both as-cast and forged specimens.

Keywords: Deformation; Stress; Strain rate; Processing map

1. Introduction

Ti-8Ta-3Nb is developed as a candidate material for applications in the human body. Compared with conventional Ti alloys it offers an improved high biocompatibility.

For successful application of Ti alloy, it is necessary to develop suitable and economical processing techniques to produce material with the desired shape without losing the low cost advantage. For designing a suitable processing route and for optimizing the hot workability, it is essential to characterize the flow stress behavior of this alloy. Such a study will also help in evaluating the mechanisms of hot deformation and achieving microstructural control in processing [1]. Different approaches available for optimizing the hot workability and evaluating the hot working mechanisms have been reviewed recently [2], including examination of shapes of stress-strain curves, evaluating kinetic parameters and developing processing maps. The present study aims at assessing the hot workability of as-cast and forged Ti-8Ta-3Nb using the approach of processing maps and comparing specimens of Ti-8Ta-3Nb. The maps are an explicit representation of the various processes that occur in the different temperature and strain rate conditions. The construction of the maps is based on the experimentally determined changes of strain rate sensitivity coefficient. They are interpreted on the basis of the principle of the dynamic materials model (DMM), which has been reviewed in papers [3-6]. In this model, the work-piece subjected to hot deformation is assumed to be a nonlinear dissipater of power. The energy transactions occurring in the work-piece consist of two parts: G content representing the dissipation by plastic work, most of which is converted into heat; the little remaining power is stored as lattice

*Corresponding author. Tel.: +82 62 530 0246, Fax.: +82 62 530 1689
E-mail address: leekw3@hanmail.net
DOI 10.1007/s12206-008-0106-5

defects and J co-content representing the dissipation through microstructure changes. The total input power is partitioned between these two as decided by the strain rate sensitivity of flow stress (m). The power dissipation map represents the manner in which the power is dissipated by the material through metallurgical processes and is constructed by plotting is-contours of dissipation efficiency (η) on a two-dimensional plot with log strain rate ($\dot{\varepsilon}$) and temperature (T) as the axes. The parameter η represents the constitutive response of the material in terms of various microstructural mechanisms that operate under given temperature and strain rate and is given by

$$\eta = \frac{2m}{m+1} \tag{1}$$

The variation of η with temperature and strain rate constitutes a power dissipation map exhibiting different domains, which may be directly correlated with specific microstructural mechanisms. The safe hot deformation mechanisms are dynamic recrystallization (DRX), dynamic recovery and superplasticity while wedge cracking and void formation at hard particles are damage processes. Acicular perform structures deformed at elevated temperatures exhibit the process of spheroidization, which occurs by the shearing of the lamellae and globularization. This process is considered to be a type of DRX [2]. The extremum principles of irreversible thermodynamics as applied to large plastic flow [7] are applicable to dynamic materials models. Kalyan Kumar [8] and Prasad [5] combined these principles with those of separability of power dissipation and obtained a continuum criterion for obtaining flow instability during hot deformation, given by:

$$\xi(\dot{\varepsilon}) = \frac{\delta \ln[m/(m+1)]}{\delta \ln \dot{\varepsilon}} + m < 0 \tag{2}$$

The variation of dimensionless parameter $\xi(\dot{\varepsilon})$ with temperature and strain rate constitutes an instability map. In this map, the temperature and strain rate regimes where ξ is negative representing microstructural instabilities. Typical microstructural manifestations of flow instabilities are adiabatic shear bands formation, flow localization, dynamic strain aging, mechanical twinning and kinking or flow rotations [6]. A superimposition of the instability map on the power dissipation map results in a processing map, which reveals the deterministic domains where individual microstructural processes occur and the limiting conditions for the regimes of flow instability. By processing under conditions of highest efficiency in the "safe" domains and by avoiding the regimes of flow instabilities, the intrinsic workability of the material may be optimized and microstructural control may be achieved. Processing maps for a wide variety of engineering materials including superalloys, intermetallics and metal-matrix composites have been compiled [4]. Comparative studies are few on deformation behavior during hot forging in as-cast and forged specimens. The present work is a comparative study on deformation behavior during hot forging in as-cast and forged specimens of Ti-8Ta-3Nb.

2. Experimental

Ti-8Ta-3Nb alloy was three times melted by VAR process. The three times melted ingot was thermomechanically processed into rods of 14 mm diameter. The initial breakdown of the ingot was followed by hot forging in the β phase field (around 950℃ [10]). The chemical composition of the alloy in wt.% was as follows: Ta-7.23, Nb-3.22, Ti-balance. The cylindrical specimens of length 8.25mm, and diameter 5.5mm, were machined from a Ti-8Ta-3Nb alloy on which homogenizing treatment was performed. Hot compression tests were carried out on both as-cast and forged specimens in the temperature range 650 - 900℃ and strain rate range from 0.001–10s^{-1}. A computer-controlled servohydraulic testing machine (Thermecmastor_Z) was used for hot compression tests. All the tests were carried out under isothermal conditions with temperature being maintained within ±2℃. The temperature of the specimen during compression tests was monitored with a thermocouple spot-welded on the surface at the height of the specimen. The flow stress values were obtained as a function of temperature, strain rate and strain. Processing maps were generated from the data obtained from the experiments [4].

3. Results and discussion

The stress-strain curves, plotted as a function of temperature at 0.1 s^{-1} and 10 s^{-1} are shown in Fig. 1. The stress-strain curves pertaining to specimens deformed at low temperature exhibited some flow softening and at high temperature the typical curves of dynamic recovery processes since the rate of work

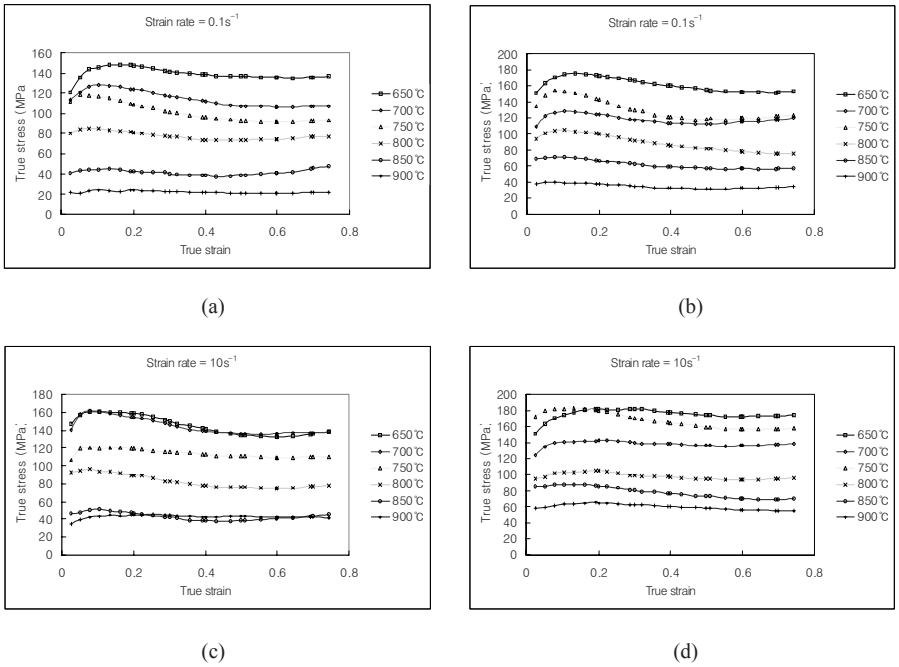

Fig. 1. True stress-strain curves of Ti-8Ta-3Nb at 0.1 s^{-1} and 10 s^{-1} for different temperatures ((a, c) as-cast specimen, (b, d) forged specimen).

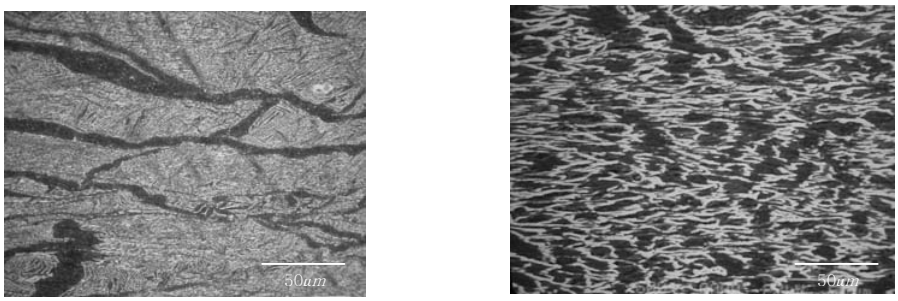

(a) At 10 s^{-1} 650℃ (as-cast) (b) At 10 s^{-1} 650℃ (forged)

Fig. 2. Microstructures of Ti-8Ta-3Nb alloy deformed at 10 s^{-1} and 650℃ (a) as-cast specimen (b) forged specimen.

hardening decreases with increasing strain. The flow stress of the forged specimens showed higher than that of the as-cast specimen over the temperatures and strain rates.

Fig. 2(a) was obtained at 10 s^{-1} and 650℃ in the as-cast specimen exhibiting some flow softening curve and Fig. 2 (b) in forged specimen exhibiting the typical curves of the dynamic recovery process. The fine microstructures which can be shown in the dynamic recrystallization process are shown partly in Fig. 2(a). But these fine microstructures in part with the local shear cannot assure that this is in a good domain for hot working. The flow softening of forged specimen at 10 s^{-1} and 650℃ in Fig. 2(b) can be attributed to the occurrence of dynamic spheroidization of the α grains or dynamic recovery [11].

Processing maps obtained at strains of 0.2, 0.3, 0.4 and 0.5 in both as-cast and forged specimens are shown in Fig. 3. The numbers against each contour represent the efficiency of power dissipation as percent. The microstructural evolution of the system with hot deformation may be tracked by following the changes in the processing maps as a function of strain. At the start of the plastic deformation, the different temperature and strain rate combinations generate a spectrum of dissipative energy states. With further

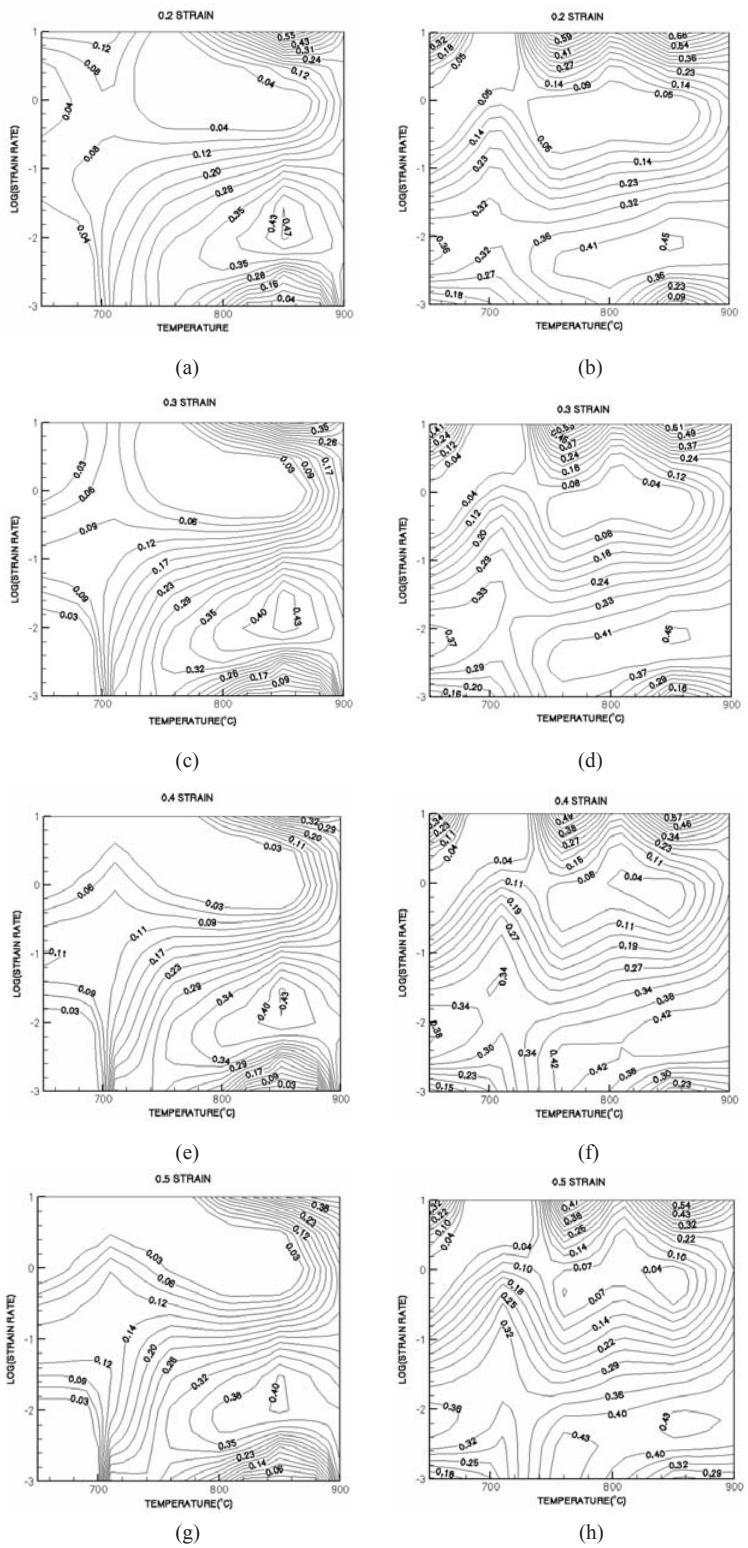

Fig. 3. Processing map for Ti-8Ta-3Nb at a strain 0.2-0.5 showing efficiency contours in a temperature-strain rate frame ((a, c, e, g) as-cast specimen, (b, d, f, h) forged specimen).

deformation, the dissipative energy states will self-organize into microstructural trajectories that go through transients before settling down or decaying into attractors sets or spaces to form domains within which the efficiency of power dissipation reaches a peak [12].

The map of as-cast specimen corresponding to a strain of 0.2 exhibits two domains spread over the temperature range of 800 to 900℃ and strain rate of $10s^{-1}$ with an efficiency of about 55% and 780 to 900℃, $0.01s^{-1}$ with an efficiency of about 47%. With further deformation to strains up to 0.5 (Fig. 3(g)), the peak efficiency of the first domain has decreased to a steady state value of about 38%; the efficiency in the region of the second domain has also decreased. The map of a forged specimen corresponding to a strain of 0.2 exhibits three domains spread over the temperature range of 720 to 800℃ and strain rate of $10s^{-1}$ with an efficiency of about 59% and 800 to 900℃, $10s^{-1}$ with an efficiency of about 58% and 740 to 900℃, $0.01s^{-1}$ with an efficiency of about 45%. With further deformation to strains up to 0.5 (Fig. 3(h)), the efficiency in the region of three domains has decreased and the third domain has split in two, one centered at 760℃ and $0.001s^{-1}$ and another one centered at 860℃ and about $0.01s^{-1}$.

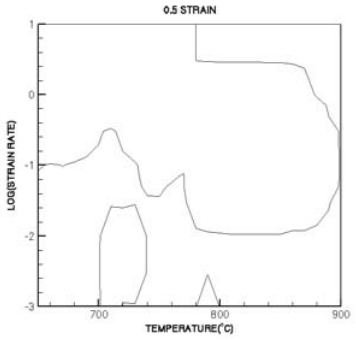

(a)

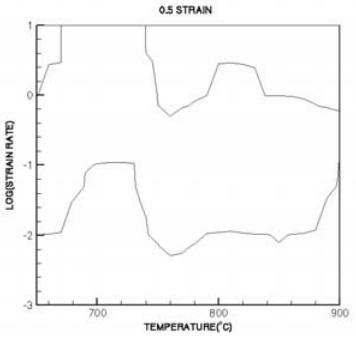

(b)

Fig. 4. Instability map developed for Ti-8Ta-3Nb at a strain of 0.5 showing contours of constant $\xi(\dot{\varepsilon})$ expressed in percent ((a) as-cast specimen, (b) forged specimen). Instability is predicted when $\xi(\dot{\varepsilon})$ is negative.

The maps of the as-cast and forged specimen have some similar contours. The maximum efficiency decreases with increasing strains in both the as-cast and forged specimen. The low efficiency area in the forged specimen is smaller than in the as-cast specimen. The efficiency of the forged specimen is higher than that of the as-cast specimen over all the ranges. The initial breakdown of the ingot increases the efficiency of the hot working. Fig. 3 shows that the efficiency contour of the as-cast and the forged specimen does not specially change with increase strain different from that of ETP copper [12].

The instability map developed on the basis of the instability criterion given by Eq. (2), corresponding to a strain of 0.5 is shown in Fig. 4. Instability maps for all other strains are similar to this in all respects as in the study by Prasad et al. [13]. The map reveals that flow instability of as-cast specimen will occur in the temperature range 650-900℃ at strain rates higher than about $0.01s^{-1}$ since $\xi(\dot{\varepsilon}) < 0$. The microstructure of the as-cast specimen deformed at 650℃ and $10s^{-1}$ is shown in Fig. 2(a), which exhibits the local shear oriented with respect to the compression axis. And the instability map of the as-cast specimen shows this domain is in the instable range. At the temperature range 650-900℃ and strain rates over $0.01s^{-1}$ the instability regime of the forged specimen is predicted. The microstructure of the forged specimen deformed at 650℃ and $10s^{-1}$ is shown in Fig. 2(b). And the instability map of the forged specimen shows this domain is in the stable range. Thus, the above microstructure observations validate the continuum instability criterion.

4. Conclusions

The hot workability of as-cast and forged specimens of Ti-8Ta-3Nb is evaluated by using the power dissipation maps developed on the basis of the dynamic materials model. The flow stress of the forged specimens showed higher than that of the as-cast specimen over the temperatures and strain rates. The maps of as-cast and forged specimens have some similar contours. The maximum efficiency decreased with increasing strains in both as-cast and forged

specimens. The efficiency of the forged specimen was higher than that of as-cast specimen over all the ranges. The initial breakdown of the ingot increased the efficiency of a hot working. The efficiency contour of as-cast and forged specimen does not especially change with increased strain. The map reveals that flow instability will mainly occur in the temperature range 650-900℃, at strain rates higher than about $0.01s^{-1}$ in both as-cast and forged specimens. The microstructure observations validated the continuum instability criterion.

References

[1] R. S. Sundar and D. H. Sastry, Y. V. R. K. Prasad, Hot workability of as-cast Re3Al-2.5%Cr intermetallic alloy, *Materials Science and Engineering* A347 (2003) 86-92.

[2] Y. V. R. K. Prasad and T. Seshacharyulu, Modeling of hot deformation for microstructural control, *Int. Mater*. Rev. 43 (1998) 243.

[3] H. L. Gegel, J. C. Malas, S. M. Doraivelu and V. A. Schende, Metals Handbook, ninth ed., ASM, Metals Park, OH, (1987) 417.

[4] Y. V. R. K. Prasad, S. Sasidhara (Eds.), Hot Working Guide: A Compendium of Processing Maps, ASM International, Materials Park, OH, (1997).

[5] Y. V. R. K. Prasad, Recent advances in the science of mechanical processing, *Indian J. Technol.* 28 (1990) 435.

[6] Y. V. R. K. Prasad, T. Seshacharyulu, Processing maps for hot working of titanium alloys, *Materials Science and Engineering* A243 (1998) 82-88.

[7] H. Ziegler, in: I. N. Sneddon, R. Hill (Eds.), *Progress in Solid Mechanics*, vol. 4, North Holland, Amsterdam, (1963) 93-193.

[8] A. K. S. Kalyand Kumar, Criteria for predicting metallurgical instabilities in processing, MSc (Eng) Thesis, Indian Institute of Science, Bangalore, India, (1987).

[9] Y. V. R. K. Prasad, *Ind. J. Technol*. 28 (1990) 435.

[10] Kyung Won Lee, Jae Sam Ban, Yeong Seon Yu and Kyu Zong Cho, A Study on the Mechanical Properties of Ti-8Ta-3Nb Alloy for Biomaterials, *KSME International Journal*, Vol. 18, No. 12 (2004) 2204-2208.

[11] N. K. Park, J. T. Yeom and Y. S. Na, Characterization of deformation stability in hot forging of conventional Ti-6Al-4V using processing maps, *Journal of Materials Processing Technology* 130-131 (2002) 540-545.

[12] Y. V. R. K. Prasad and K. P. Rao, Processing maps and rate controlling mechanisms of hot deformation of electrolytic tough pitch copper in the temperature range 300-950℃, *Materials Science and Engineering A*, Vol. 391 (2005) 141-150.

[13] Y. V. R. K. Prasad, S. Sasidhara and V. K. Sikka, Characterization of mechanisms of hot deformation of as-cast nickel aluminide alloy, *Intermetallics* 8 (2000) 987-995.